Complement activation in vitro and reactogenicity of low-molecular weight dextran-coated SPIONs in the pig CARPA model: Correlation with physicochemical features and clinical information

Tamás Fülöp[a,e,1], Réka Nemes[b,1], Tamás Mészáros[a], Rudolf Urbanics[c], Robbert Jan Kok[b], Joshua A. Jackman[d], Nam-Joon Cho[d], Gert Storm[b,e,1], János Szebeni[a,c,f,*]

[a] Nanomedicine Research and Education Center, Dept. Pathophysiology, Semmelweis University, Budapest, Hungary
[b] Dept. Pharmaceutics, Utrecht Institute for Pharmaceutical Sciences, Utrecht University, PO Box 80082, 3508 TB Utrecht, The Netherlands
[c] SeroScience Ltd, Budapest, Hungary
[d] School of Materials Science and Engineering, Nanyang Technological University, 50 Nanyang Drive, 637553, Singapore
[e] Dept. Targeted Therapeutics, MIRA Institute, University of Twente, PO Box 217, 7500 AE Enschede, The Netherlands
[f] Dept. Nanobiotechnology and Regenerative Medicine, Faculty of Health, Miskolc University, Budapest, Hungary

ARTICLE INFO

ABSTRACT

The unique magnetic properties of superparamagnetic iron oxide nanoparticles (SPIONs) have led to their increasing use in drug delivery and imaging applications. Some polymer-coated SPIONs, however, share with many other nanoparticles the potential of causing hypersensitivity reactions (HSRs) known as complement (C) activation-related pseudoallergy (CARPA). In order to explore the roles of iron core composition and particle surface coating in SPION-induced CARPA, we measured C activation by 6 different SPIONs in a human serum that is known to react to nanoparticles (NPs) with strong C activation. Remarkably, only the carboxymethyldextran-coated (ferucarbotran, Resosvist®) and dextran-coated (ferumoxtran-10, Sinerem®) SPIONs caused significant C activation, while the citric acid, phosphatidylcholine, starch and chitosan-coated SPIONs had no such effect. Focusing on Resovist and Sinerem, we found Sinerem to be a stronger activator of C than Resovist, although the individual variation in 15 different human sera was substantial. Further analysis of C activation by Sinerem indicated biphasic dose dependence and significant production of C split product Bb but not C4d, attesting to alternative pathway C activation only at low doses. Consistent with the strong C activation by Sinerem and previous reports of HSRs in man, injection of Sinerem in a pig led to dose-dependent CARPA, while Resovist was reaction-free. Using nanoparticle tracking analysis, it was further determined that Sinerem, more than Resovist, displayed multimodal size distribution and significant fraction of aggregates – factors which are known to promote C activation and CARPA. Taken together, our findings offer physicochemical insight into how key compositional factors and nanoparticle size distribution affect SPION-induced CARPA, a knowledge that could lead to the development of SPIONs with improved safety profiles.

1. Introduction

Superparamagnetic iron oxide nanoparticles (SPIONs), state-of-art representatives of clinically useful nanoparticles (NPs), have been used as contrast agents for magnetic resonance imaging (MRI) over the past decade [1–5]. They are in the 10–100 nm range (up to 30 nm in the case of USPIONs) and contain a γ-Fe_2O_3 (maghemite), Fe_3O_4 (magnetite) or α-Fe_2O_3 (hermatite) core and a hydrophilic surface coating made from a variety of polymers, including dextran, carboxydextran, chitosan, phospholipids, polyethylene glycol (PEG) and starch. The iron core lends these particles "superparamagnetism", in essence external magnetic field-controllable magnetism that enables these particles to be utilized for imaging, molecular structure analysis or to the benefit of drug delivery, gene therapy and many other

potential applications [6–8].

Among the unsolved challenges of the clinical application of many iron-containing drugs and contrast media is that they can cause hypersensitivity reactions (HSRs). The symptoms of HSRs reported for reactogenic iron-compounds include dyspnea, chest/back pain, hypo/hypertension, fever, flushing, rash and panic, that are also typical symptoms of the HSRs to liposomal and micellar drugs, biological therapeutics, radiocontrast agents, enzymes, PEGylated proteins and many other "nanobiopharmaceuticals". These reactions were proposed to be due, at least in part, to activation of the complement (C) system, leading to the term "C activation-related pseudoallergy (CARPA) [9–13]. The worst outcome of CARPA is anaphylaxis with occasional death, which contributed to market withdrawal of ferumoxide (Feridex/Endorem®) [14], ferumoxytol (Feraheme®/Rienso®) [15] and ferumoxtran (Ferumoxtran-10/Sinerem/Combidex) [16].

As implied in its name, the essence of CARPA is the capability of the drug or agent to cause C activation. Such activation has been shown for many of the above listed CARPAgenic drugs [10] including 20-kD dextran-coated SPIONs called "nanoworms" [19–23]. These $FeCl_2$/$FeCl_3$ precipitates with multiple crystalline cores were shown to activate all 3 (classical, alternative and lectin) pathways in human serum [23], highlighting the redundancy of C activating triggers. Likewise, a recent study reported C activation by iron dextran and ferric carboxymaltose both in vitro and in vivo in the blood of healthy volunteers and hemodialysis patients, leading to the conclusion that HSRs to these drugs could represent CARPA [24]. In fact, the concept that CARPA may underlie many HSRs to iron-containing drugs is gaining increasing attention [25], motivating further exploration of the C reactivity and CARPAgenic activity of SPIONs.

Accordingly, the first goal of our study was to measure C activation by different SPIONs in vitro, and to identify the structural factors responsible for such activation. Having found that only the dextran coat caused C activation, we went further to compare different dextran-coated SPIONs, including low molecular weight (10 kDa) dextran-covered ferumoxtran-10 (Sinerem®) and low-molecular weight (MW:548) carboxydextran-coated ferucarbotran (Resovist®) for which information on the HSRs they caused in patients allowed us to correlate the in vitro and animal data obtained in this study with the past human observations.

2. Materials and methods

2.1. Materials

Superparamagnetic iron-oxide nanoparticles (SPIONs) with different surface coatings (FluidMAG-chitosan, -starch, -phosphatidylcholine, -dextran, -carboxymethyldextrane, and -citric acid) were obtained from Chemicell GmbH (Germany). SPIONs approved for clinical use (Sinerem® and Resovist®) were kindly offered by Nano4Imaging GmbH (Germany). Sinerem and Resovist have dextran and carboxydextrane coatings, respectively, but in absence of structural information about their similarity to FluidMAG-dextran and -carboxymethyldextrane, all these NPs are considered as distinct test agents. Quidel's SC5b-9, Bb and C4d C ELISAs were obtained from TECOmedical NL (The Netherlands). Zymosan was obtained from Sigma-Aldrich. Mixed breed male Yorkshire/Hungarian White Landrace pigs (2–3 months old, 18–22 kg) were obtained from the Animal Breeding and Nutrition Research Institute, Herceghalom, Hungary.

2.2. Methods

2.2.1. Measurement of complement activation in human serum in vitro

Sera from healthy volunteers were incubated with the tested polymers and SPIONs for 30 min at 37 °C at a serum/nanoparticle volume ratio of 4:1, duplicate tubes. The iron content of particles was matched. Incubation was stopped by diluting the samples with EDTA containing sample diluent from the ELISA kits, and aliquots from these diluted sera were subjected to measuring SC5b-9, Bb and C4d as pathway specific markers of C activation [26,27]. In addition we also applied a modified hemolytic C (CH50) assay, as described earlier [28]. In short, the nanoparticles were incubated with the sera at 37 °C for 30 min followed by a 10-fold dilution in PBS. Aliquots from these diluted sera were incubated with sensitized sheep red blood cells (SRBCs) for 10 min at 37 °C. The reaction was stopped by centrifugation of the cells at 4 °C and measurement of released hemoglobin at 541 nm. The readings were expressed as % of maximal hemolysis in saline control, and C consumption was obtained by 100% minus % hemolyis.

2.2.2. In vivo test of CARPA in pigs

Resovist and Sinerem were tested for CARPA in pigs, according to a procedure described previously [13,29–32]. In brief, animals were sedated with Calypsol/Xilazine and then anesthetized with isoflurane (2–3% in O_2). Intubation was performed with endotracheal tubes to maintain free airways, and to enable controlled ventilation if necessary. The animals were breathing spontaneously during the experiments. In order to measure the pulmonary arterial blood pressure (PAP), a Swan–Ganz catheter (Teleflex Medical, Research Triangle Park, NC, USA) was placed to the pulmonary artery wedge. Additional catheters were placed into the femoral artery to record the systemic arterial pressure (SAP). The left femoral vein was cannulated for blood sampling, and the external jugular vein for the administration of SPIONs. The hemodynamic parameters were measured continuously.

2.2.3. Characterization of nanoparticles
2.2.3.1. Size and zeta potential measurements. The mean diameter and size distribution (polydispersity index, PDI) of SPIONs were determined by dynamic light scattering (DLS) with Malvern ALV CGS-3 system (Malvern instruments Ltd., Malvern, Worcestershire, United Kingdom) with a scattering angle of 90° at 25 °C. Samples were diluted 200 times using pure 18.2 MΩ cm distilled (Milli-Q, Millipore, Molsheim, France) water before measurement.

The zeta-potential was measured by laser Doppler electrophoresis using Zetasizer Nano-Z (Malvern instruments Ltd., Malvern, Worcestershire, United Kingdom). The nanoparticles were diluted approximately 100 times in 10 mM HEPES (pH 7.4) before measurement.

2.2.3.2. Nanoparticle tracking analysis (NTA). Nanoparticle tracking analysis was conducted with a Nanosight LM10 instrument. The particles were diluted to a concentration of 5 µg/mL in Milli-Q-treated water. A 405 nm laser was used to illuminate and cause Rayleigh scattering by the particles, which was visualized by optical microscope (20 × magnification). The time-resolved Brownian motion of individual particles was recorded by camera for a time period of 60s at a rate of 25 frames per second, enabling the calculation of the hydrodynamic diameter of individual particles by the two-dimensional Stokes-Einstein equation and construction of a number-weighted size histogram. Video capture and data analysis parameters were controlled using the NTA 3.1 software program. All measurements were carried out under room temperature of 24 °C.

2.2.4. Statistical analysis
Comparisons of multiple groups were made by ANOVA followed by Tukey's Multiple Comparison Test, with P < 0.05 taken a significant difference.

3. Results and discussion

3.1. Physicochemical characterization of iron-NPs

Table 1 shows some physicochemical properties and other specifics of iron NPs used in this study. The diameters specified represent the mean values obtained by DLS (See Methods).

Table 1
Physicochemical properties of different SPIONs used in this study.

Core	Coating/vehicle	Generic name	Trade name	Diameter (nm)/PDI	Zeta Pot. (mV)	Manufacturer
Experimental						
Fe_3O_4	Citric acid	–	FluidMAG-CT	140/0,2	− 35,9	Chemicell GmbH
	Phosphatidylcholine	–	FluidMAG-Lipid	189/0,3	− 33	
	Starch	–	FluidMAG-D	40/0,1	− 9.7	
	Chitosan	–	FluidMAG-Chitosan	68/0,2	4,7	
Clinically used (discontinued)						
Fe^{3+}/Fe^{2+}	Carboxydextran	Ferucarbotran	Resovist® (EU) Cliavist® (US)	60.6/0,2	− 26,4	Bayer Shering Pharma AG
	Dextran	Ferumoxtran-10	(Sinerem®, EU) Combidex® (US)	50.7/0,3	− 13,8	Guerbet, Advanced Magnetics

Abbreviations in the Table: PDI, polydispersity index, Pot, potential.

3.2. Complement activation by different SPIONs in a sensitive human serum

Previous studies on nanomedicine-induced C activation in normal (healthy) human sera in vitro and patients in vivo showed substantial individual variation, with 1–10% of humans being highly reactive for specific nanodrugs [33–40]. This variation has not been understood to date, thus, as a useful step in experiments comparing C activation by NPs, we have chosen a serum which gave strong C activation in vitro in previous experiments (mainly by liposomal doxorubicin, Doxil [37]). Fig. 1A–C shows C activation in this preselected reactive serum by SPIONs with different cores and surface coatings at 3 different concentrations: 0.1, 0.5 and 10 mg/mL iron (panels A–C, respectively). Nanoparticles with chitosan and phosphatidylcholine coatings were

reaction free at all doses, those with starch and carboxymethyldextran caused minor C activation, while iron NPs with dextran coating caused massive activation. Regarding the dose-dependence of these effects, there is ~25–30% rise in C activation by carboxymethyldextran and dextran in panel B versus panel A, suggesting that 0.1 and 0.5 mg/mL iron were within the dynamic range of the dose-effect relationship for these SPIONs. Surprisingly, the C activating effect of dextran-coated NPs showed biphasic dose-dependence as 0.1 and 0.5 mg/mL were stimulatory, while 10 mg/mL was inhibitory. Fig. 1D shows an independent experiment in which we looked at C activation by 0.14–1.38 mg/mL free 10 kDa dextran. This concentration range embraces the dextran content of dextran-SPIONs applied at 10 mg iron/mL (0.63 mg/mL, see legend to Fig. 1), which had suppressive effect on C
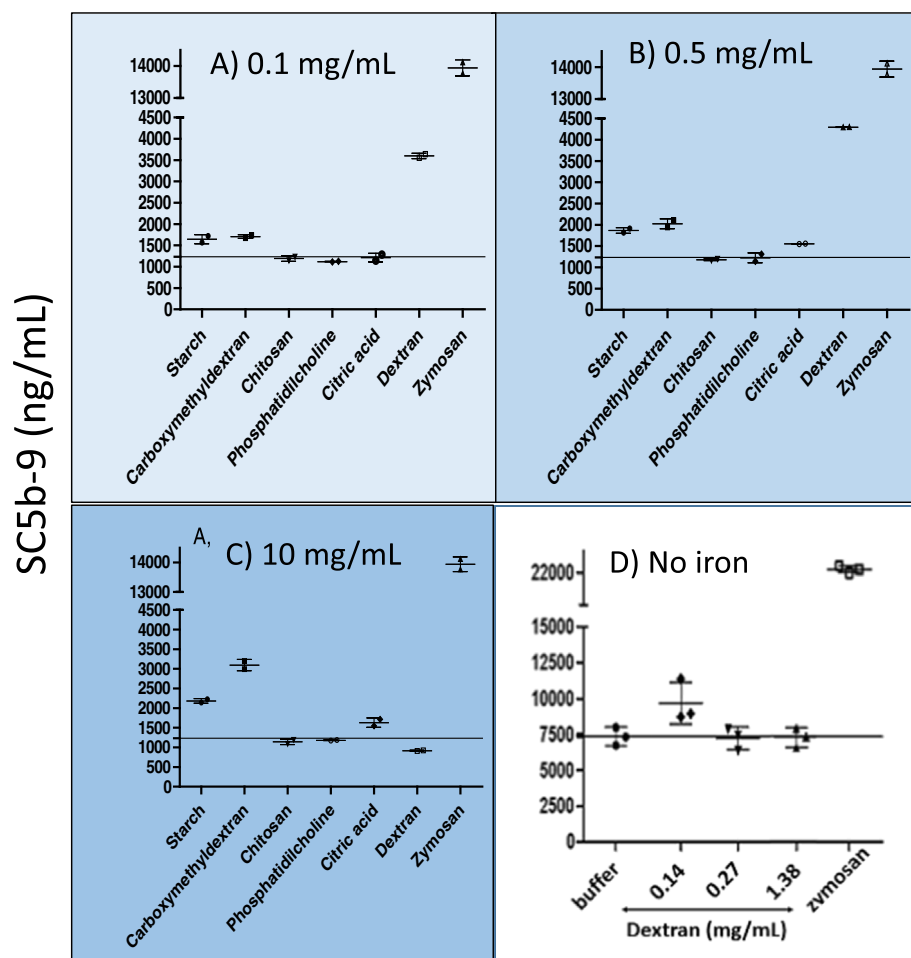
Fig. 1. Complement activation by different SPIONs (Panels A–C) and free dextran (D) in a preselected "sensitive" NHS after incubation for 30 min at 37C. Panels A–C show the dose dependence of activation by FluidMAG SPIONS coated with starch, carboxymethyldextrane, chitosan, phosphatidylcholine, citric acid and dextran (X axis). The final concentration of each NP was adjusted to the iron content specified at the top of each panel. The horizontal line shows the PBS baseline of SC5b-9. Panel D shows an independent experiment wherein the serum was incubated with free dextran (10 kDa, the same as used in Sinerem) at doses specified in mg/mL dextran. The error bars represent SD of duplicate measurements (n = 2). Conversion between the iron and coating polymer concentrations was made for FluidMAG dextran on the basis of product information, giving an iron/polymer ratio of ~16. Thus, the polymer concentrations in FluidMAG-dextran NPs were ~6, 30 and 600 ng/mL in panels A–C, respectively.

activation. Remarkably, free dextran also displayed inverse dose-effect relationship, with suppressed C activation at doses > 0.14 mg/mL. These data suggest that depending on concentration, dextran can activate or inhibit C activation both in free and in NP-bound form. The underlying reason for this phenomenon is not understood at this time, nor are the observations on less intense C activation by starch-, carboxymethyldextran- and citrate-containing SPIONs. Unlike dextran-SPIONs, the dose-effect relationship with these SPIONs was clearly dose dependent up to at least 10 mg/mL iron.

Taken together, these data suggest that in certain sensitive individuals certain SPIONs can activate C while others do not. The concentration dependence of C activation may vary from SPION to SPION, at it can also be biphasic, for example the case of dextran.

3.3. Complement activation by Sinerem and Resovist in normal human sera: individual variation

The above data turned our attention to two clinically approved MRI imaging SPIONs; the dextran-coated Sinerem and carboxydextran-coated Resovist (other names shown in Table 1). Here, rather than using one "sensitive" serum, we investigated the individual variation of their C activation in several NHS. As shown in Fig. 2A, incubation of Sinerem with 5 different NHS tended to lead to greater rise of SC5b-9 over baseline than that caused by Resovist, as the number of reactive sera was higher in the former group.

Questioning the inter-experimental variation of the individual variation of Sinerem-induced C activation in NHS, we tested yet another independent series of different sera and repeated the same experiment as shown in Fig. 2A, using this time 10 sera and zymosan as positive control. As shown in Fig. 2 B, the range and variation this time was
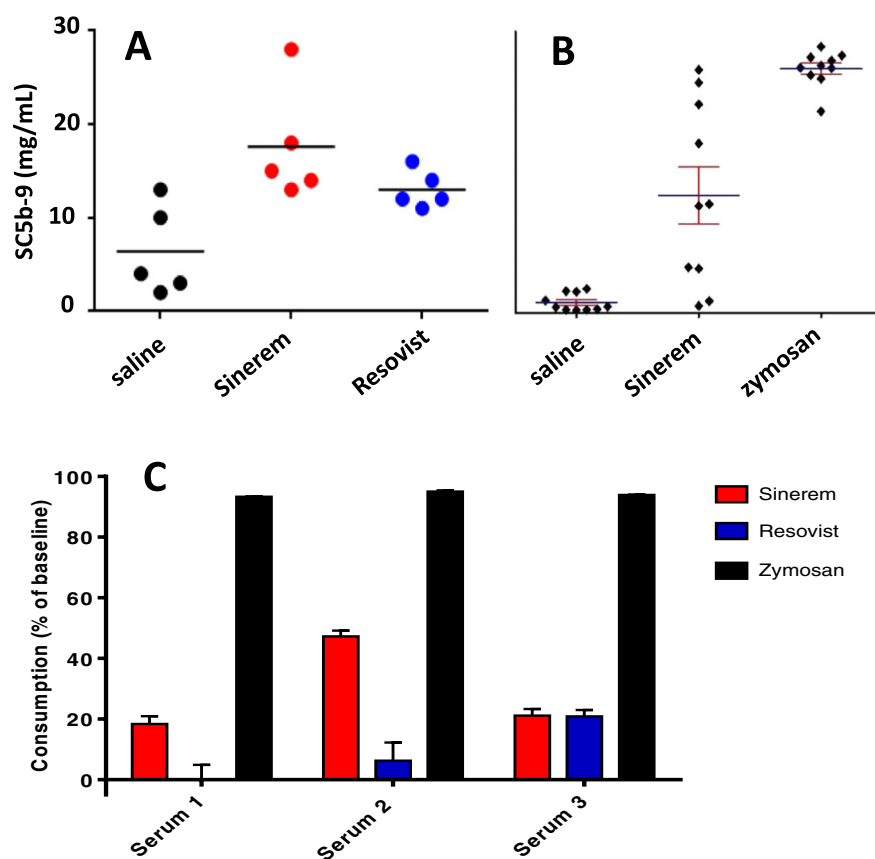
greater than in Panel A, but the basic message is the same: Sinerem activates human C with substantial individual variation. Based on this series, 8 of 10 (80%) of sera showed reactivity against Sinerem, and 3 in 10 showed activation comparable to that caused by 0.1 mg/mL zymosan.

SC5b-9 is a soluble end-product of C activation, whose individual variation may have reasons independent of the central reaction, i.e. C3 conversion and subsequent cascadic formation of the terminal complex (C5b-9). For this reason, we also evaluated the effects of Sinerem and Resovist on the whole C cascade by using a modified hemolytic assay which measured the consumption of all C proteins that are involved in hemolysis (hemolytic C). Fig. 2C shows greater consumption of hemolytic C by Sinerem than Resovist in 2 of the 3 tested sera, and this finding is consistent with the conclusions drawn from the SC5b-9 ELISA. Thus, the differential effects of tested SPIONs apply to the whole C cascade.

3.4. Pathway of complement activation by Sinerem

In order to determine the pathway of C activation by Sinerem we incubated 3 different NHS with Sinerem and measured the production of SC5b-9, C4d and Bb, which are specific markers of the terminal, classical and alternative pathways, respectively. The significant and comparable elevations of SC5b-9 and Bb (Fig. 3) clearly indicate the involvement of alternative pathway activation, with no, or negligible operation of the classical pathway.

3.5. CARPAgenic activity of Resovist and Sinerem in pigs

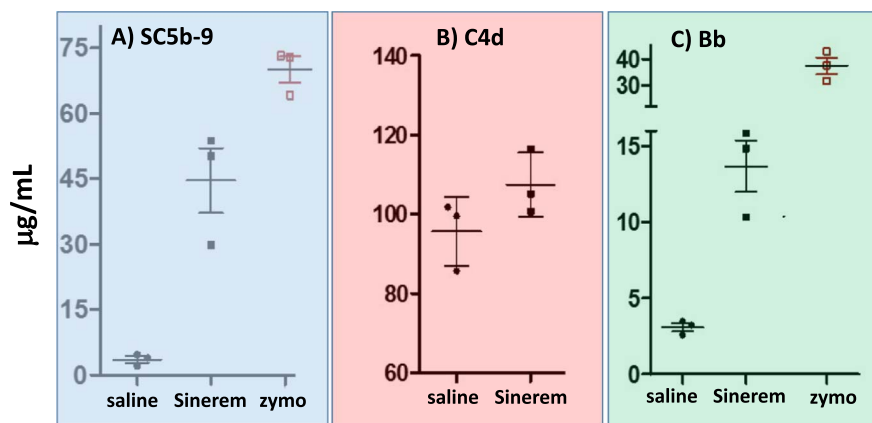The above in vitro data indicating quantitative differences in C

Fig. 2. Complement activation by Sinerem and Resovist under different experimental conditions. In A, 5 different NHS were incubated with Sinerem and Resovist (0.25 mg/mL iron, ~16 ng/mL dextran) and in B, a different set of 10 NHS was incubated with Sinerem (0.25 mg/mL iron or 0.1 mg/mL zymosan. In the latter experiment ANOVA followed by Tukey's Multiple Comparison Test showed the 3 groups significantly differing from each other (P < 0.05). Panel C shows the results of a hemolytic assay, testing C consumption by Sinerem, Resovist and zymosan at the same levels as in A and B. The sheep red cell assay was described in the Methods. Bars are mean ± SD for duplicate measurements in each sera.

Fig. 3. Pathway of C activation by Sinerem tested in 3 NHS. Panels A-C show the results of SC5b-9, C4d abd Bb ELISA performed in 3 NHS. Sinerem and zymosan (Zymo) were applied at 0.25 and 0.1 mg/mL, respectively. Bars are mean ± SD for duplicate measurements in each sera.

activation by Resovist and Sinerem led to a critical question: do these differences entail differential biological responses in an animal model of CARPA? Or more broadly: can in vitro C measurements predict HSRs?

To address this question, we used the porcine CARPA model, which is known to be a sensitive quantitative assay of the acute immune reactivity of NPs manifested in anaphylactoid reactions [13,29–32]. We injected Resovist and Sinerem in consecutive boluses at 0.1 and 0.5 mg/ kg iron and traced the changes of pulmonary arterial pressure (PAP), systemic arterial pressure (SAP) and heart rate (HR) as hemodynamic endpoints of CARPA. Before these injections, a bolus of saline served as a negative (volume) control, while at the end of the experiment, zymosan served as a positive control, testifying to the intactness of the pigs' cardiovascular reactivity. As shown in Fig. 4, Resovist did not cause any changes in the measured parameters (Fig. 4A), while Sinerem

did cause significant dose-dependent changes (Fig. 4B). Namely, 0.01 and 0.1 mg/kg doses led to 30–40 and 50–60% rises in both PAP and SAP, respectively, and the response of PAP, as well as the tachycardia, were clearly more expressed at the higher dose (sub-curve area of PAP 3-fold higher, up to 25 BPM tachycardia).

3.6. Nanoparticle tracking analysis of Resovist and Sinerem

In an effort to explain the observed differences between Resovist and Sinerem in C activation and CARPA, we performed additional dynamic light scattering (DLS) and nanoparticle tracking analysis (NTA) experiments with these particular SPIONs. As shown in Fig. 5A, the DLS technique showed that Resovist NPs ranged in size from around 40 to 120 nm diameter, with 2 peaks between 40 and 60 and 70–120 nm. In
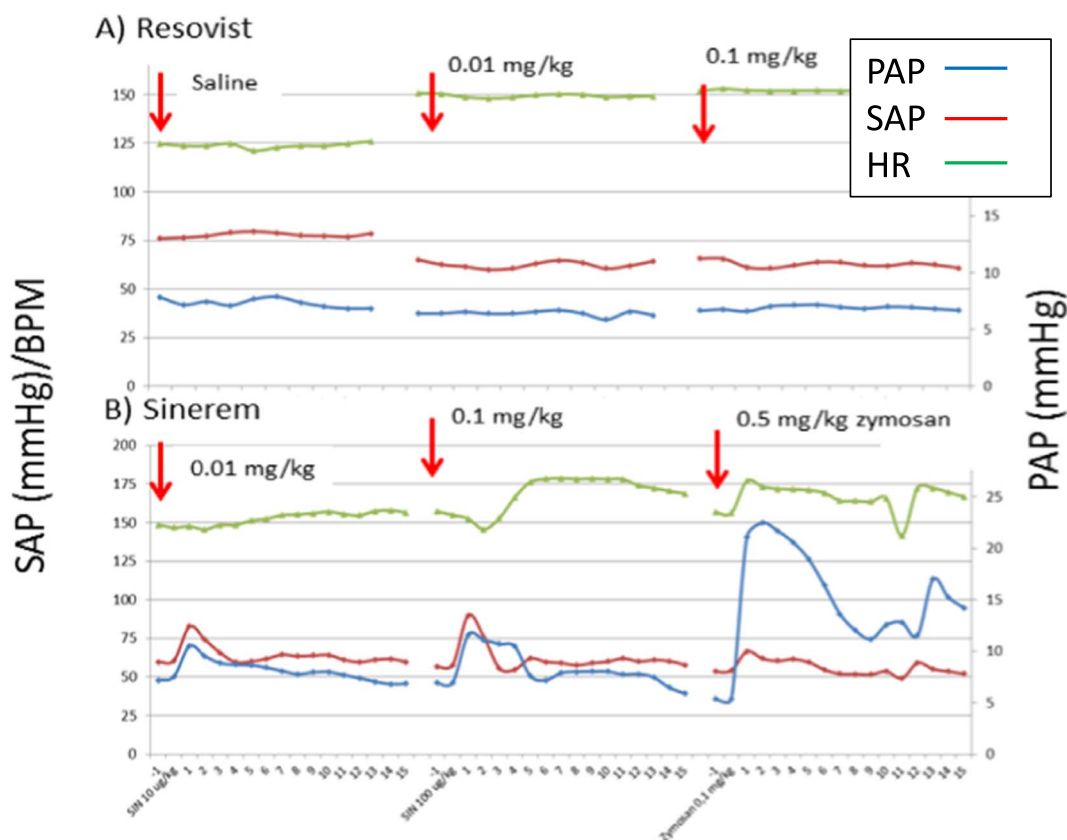

Fig. 4. Hemodynamic changes caused by Resovist and Sinerem in pigs. The changes in systemic arterial pressure (SAP, red), pulmonary arterial pressure (PAP, blue) and heart rate (beat/ min, BPM (green)) were followed up to 15 min (X-axis) shown on the x axis. (For interpretation of the references to colour in this figure legend, the reader is referred to the web version of this article.)
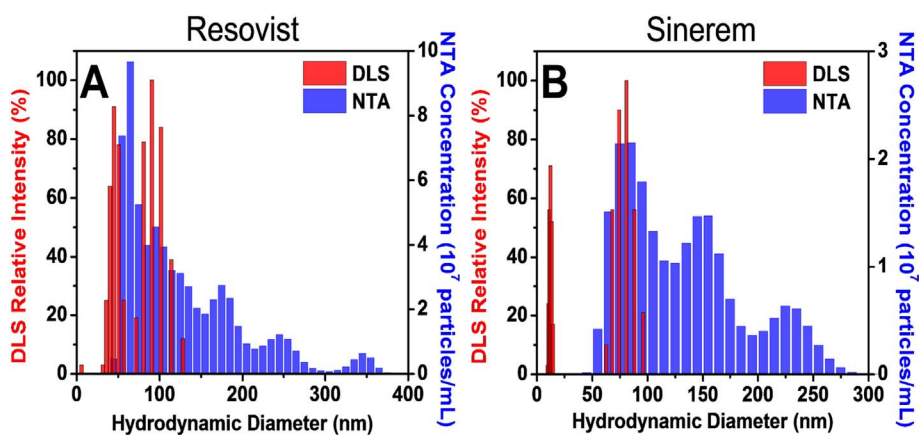
the same sample, the NTA experiment (which measures the concentration, i.e., an absolute number of NPs as a function of hydrodynamic diameter) indicated a peak at about 60 nm with gradual decline of NP number with increasing size until about 360 nm. The minor peaks superimposed on the slope of concentration curve (contour) are indicative of inhomogeneities, most likely aggregates, but these were not as expressed to such an extent as seen for Sinerem (Fig. 5B).

For Sinerem, the NTA experiment revealed major peaks around 75, 150 and 225 nm, and the DLS data were also different from that obtained with Resovist, with peaks at about 30 and 80 nm. While these values agree well with the reported size distribution of SPIONs in general [41], they also reveal quantitative differences between the two studied preparations. Namely, the NTA contour of Sinerem was skewed towards larger NPs compared to Resovist, indicating higher percentage of relatively large (> 100 nm) NPs with inhomogeneous distribution. The smaller-size population agrees well with the reported size of Sinerem particles [42], while the larger-size population probably includes aggregates. Of note, NTA has a detection limit around 30 nm and only particles above this minimum size (i.e., in this case, SPION aggregates) can be observed with this technique [43]. Taken together, the NTA measurements suggest that a possible underlying factor behind the increased C activating and CARPAgenic activity of Sinerem is the increased size and inhomogeneity of NPs in it, with possible presence of aggregates, which are known contributors to C activation and HSRs [44]. Regarding the role of aggregates, however, it needs to be pointed out that our test samples were not freshly opened original vials, and they were not filtered before application although the product insert of Sinerem, but not that of Resovist, recommends filtering of the infusate before human application to get rid of possible aggregates. Thus, aggregates may not entirely explain the clinical reactions, obviously, many other factors may also play important roles. A role of C controlling proteins, such as Factor H, should be considered, since we have shown that C activation proceeded on the alternative pathway, and Factor H is an alternative pathway inhibitor. It has a prominent polyanionic binding site [45] and thus its increased binding to the highly anionic Resovist (Table 1) may have contributed to its decreased C activation.

In summary, the focus of the present study was to, through a comparative analysis, elucidate physicochemical factors of SPIONs that may cause potentially serious HSR via C activation. Such reactions have been described for the dextran-coated SPIONs, ferumoxides [14] and ferumoxtran-10 (Combidex/(Sinerem) with frequencies in the 2–5% range [16,46,47], and this range is also typical of CARPA caused by other nanomedicines and other agents [10]. Recent credit for CARPA being the likely underlying cause of HSRs to iron-containing compounds came from an editorial by Hempel [24]. Regarding SPION reactions it seems relevant to refer to a post-marketing safety review of the FDA in 2005 [48], which gives details of 18 anaphylaxis-related sudden (within 2–30 min) deaths in recipients of various iron dextran

preparations including MRI contrast agents. The reported initial symptoms (flushing, shortness of breath, chest/back pain, dizziness, hypo/hypertension, edema, arrhythmias) as well as a cause of death (cardiac arrest) are exactly the same symptoms that are observed with other CARPAgenic drugs [10,31].

The present study confirmed the C activating capability of two dextran-containing SPIONs used in tumor diagnosis; Sinerem and Resovist. Before withdrawing from the market, Sinerem was used for MRI imaging of lymph nodes, while Resovist was a liver specific MRI contrast agent. Our data suggest stronger C activation and stronger in vivo reactivity of Sinerem compared to Resovist, which is consistent with the information that HSRs contributed to the withdrawal from the market of Sinerem [16], but not that of Resovist [17,18]. We can also correlate the C activation data with at least one particle feature known to contribute to C activation and CARPA: inhomogeneity [44]. While the DLS average size info (Table 1) showed no difference, the NTA analysis revealed more expressed inhomogeneity in Sinerem than in Resovist, which could be due to increased amounts of aggregates in the latter preparation. This possibility highlights the importance of using adequate methods for the physicochemical characterization of NPs, in the present example to quantify inhomogeneity and to detect aggregates. Nevertheless, other factors are also likely to contribute to the increased reactogenicity of Sinerem and many other therapeutic or diagnostic NPs, which will have to be explored in the future.

Acknowledgments

References

[1] R. Jin, B. Lin, D. Li, H. Ai, Superparamagnetic iron oxide nanoparticles for MR imaging and therapy: design considerations and clinical applications, Curr. Opin. Pharmacol. 18 (2014) 18–27.
[2] H.J. Kwon, W.H. Shim, G. Cho, H.J. Cho, H.S. Jung, C.K. Lee, Y.S. Lee, J.H. Baek, E.J. Kim, J.Y. Suh, Y.S. Sung, D.C. Woo, Y.R. Kim, J.K. Kim, Simultaneous evaluation of vascular morphology, blood volume and transvascular permeability using SPION-based, dual-contrast MRI: imaging optimization and feasibility test, NMR Biomed. 28 (2015) 624–632.
[3] X. Ma, A. Gong, B. Chen, J. Zheng, T. Chen, Z. Shen, A. Wu, Exploring a new SPION-based MRI contrast agent with excellent water-dispersibility, high specificity to cancer cells and strong MR imaging efficacy, Colloids Surf. B: Biointerfaces 126

(2015) 44–49.

[4] X. Mao, J. Xu, H. Cui, Functional nanoparticles for magnetic resonance imaging, Wiley Interdiscip. Rev. Nanomed. Nanobiotechnol. 8 (2016) 814–841.

[5] B. Sivakumar, R.G. Aswathy, R. Romero-Aburto, T. Mitcham, K.A. Mitchel, Y. Nagaoka, R.R. Bouchard, P.M. Ajayan, T. Maekawa, D.N. Sakthikumar, Highly versatile SPION encapsulated PLGA nanoparticles as photothermal ablators of cancer cells and as multimodal imaging agents, Biomater. Sci. 5 (2017) 432–443.

[6] A. Figuerola, R. Di Corato, L. Manna, T. Pellegrino, From iron oxide nanoparticles towards advanced iron-based inorganic materials designed for biomedical applications, Pharmacol. Res. 62 (2010) 126–143.

[7] S. Wahajuddin, Arora, Superparamagnetic iron oxide nanoparticles: magnetic nanoplatforms as drug carriers, Int. J. Nanomedicine 7 (2012) 3445–3471.

[8] H. Mok, M. Zhang, Superparamagnetic iron oxide nanoparticle-based delivery systems for biotherapeutics, Expert Opin. Drug Deliv. 10 (2013) 73–87.

[9] J. Szebeni, Complement activation-related pseudoallergy: a new class of drug-induced acute immune toxicity, Toxicology 216 (2005) 106–121.

[10] J. Szebeni, Complement activation-related pseudoallergy: a stress reaction in blood triggered by nanomedicines and biologicals, Mol. Immunol. 61 (2014) 163–173.

[11] J. Szebeni, G. Storm, Complement activation as a bioequivalence issue relevant to the development of generic liposomes and other nanoparticulate drugs, Biochem. Biophys. Res. Commun. 468 (2015) 490–497.

[12] J. Szebeni, F. Muggia, Y. Barenholz, Case study: Complement activation related hypersensitivity reactions to PEGylated liposomal doxorubicin: Experimental and clinical evidence, mechanisms and approaches to inhibition, in: M.A. Dobrovolskaia, S.E. McNeil (Eds.), Handbook of Immunological Properties of Engineered Nanomaterials, 2nd ed., World Scientific Publishing Company, 2015, pp. 331–361.

[13] J.A. Jackman, T. Meszaros, T. Fulop, R. Urbanics, J. Szebeni, N.J. Cho, Comparison of complement activation-related pseudoallergy in miniature and domestic pigs: foundation of a validatable immune toxicity model, Nanomedicine: NBM 12 (2016) 933–943.

[14] W. Bayer Healthcare Pharmaceuticals, NJ, Feridex I.V. (Ferumoxides Injectable Solution), https://www.drugs.com/pro/feridex.html, (2017).

[15] EMA, EMA Assessment Report, Rienso, http://www.ema.europa.eu/docs/en_GB/document_library/EPAR_-_Assessment_Report_-_Variation/human/002215/WC500184877.pdf, (2015).

[16] C. Advanced Magnetics Inc., Oncology, Drug Advisory Committee Biefing Doument, NDA 21-115, (2005), pp. 68–71.

[17] V.M. Runge, Safety of approved MR contrast media for intravenous injection, J. Magn. Reson. Imaging 12 (2000) 205–213.

[18] V.M. Runge, Safety of magnetic resonance contrast media, Top. Magn. Reson. Imaging 12 (2001) 309–314.

[19] G. Wang, J.I. Griffin, S. Inturi, B. Brenneman, N.K. Banda, V.M. Holers, S.M. Moghimi, D. Simberg, In vitro and in vivo differences in murine third complement component (C3) opsonization and macrophage/leukocyte responses to antibody-functionalized iron oxide nanoworms, Front. Immunol. 8 (2017) 151.

[20] F. Chen, G. Wang, J.I. Griffin, B. Brenneman, N.K. Banda, V.M. Holers, D.S. Backos, L. Wu, S.M. Moghimi, D. Simberg, Complement proteins bind to nanoparticle protein corona and undergo dynamic exchange in vivo, Nat. Nanotechnol. 12 (2017) 387–393.

[21] S. Inturi, G. Wang, F. Chen, N.K. Banda, V.M. Holers, L. Wu, S.M. Moghimi, D. Simberg, Modulatory role of surface coating of superparamagnetic iron oxide nanoworms in complement opsonization and leukocyte uptake, ACS Nano 9 (2015) 10758–10768.

[22] N.K. Banda, G. Mehta, Y. Chao, G. Wang, S. Inturi, L. Fossati-Jimack, M. Botto, L. Wu, S.M. Moghimi, D. Simberg, Mechanisms of complement activation by dextran-coated superparamagnetic iron oxide (SPIO) nanoworms in mouse versus human serum, Part. Fibre Toxicol. 11 (2014) 64.

[23] G. Wang, S. Inturi, N.J. Serkova, S. Merkulov, K. McCrae, S.E. Russek, N.K. Banda, D. Simberg, High-relaxivity superparamagnetic iron oxide nanoworms with decreased immune recognition and long-circulating properties, ACS Nano 8 (2014) 12437–12449.

[24] J.C. Hempel, F. Poppelaars, M. Gaya da Costa, C.F. Franssen, T.P. de Vlaam, M.R. Daha, S.P. Berger, M.A. Seelen, C.A. Gaillard, Distinct in vitro complement activation by various intravenous iron preparations, Am. J. Nephrol. 45 (2017) 49–59.

[25] I.C. Macdougall, K. Vernon, Complement activation-related pseudo-allergy: a fresh look at hypersensitivity reactions to intravenous iron, Am. J. Nephrol. 45 (2017) 60–62.

[26] B. Romberg, L. Baranyi, R. Bünger, W.E. Hennink, J. Szebeni, G. Storm, Initial observations on complement activation by poly(amino acid)-coated liposomes, in: B. Romberg (Ed.), Poly(amino acid)s: Next-generation Coatings for Long-circulating Liposomes, Utrecht University, Utrecht, 2007Doctoral thesis.

[27] J.M. van den Hoven, R. Nemes, J.M. Metselaar, B. Nuijen, J.H. Beijnen, G. Storm,

J. Szebeni, Complement activation by PEGylated liposomes containing prednisolone, Eur. J. Pharm. Sci. (2013).

[28] T. Mészáros, G. Szénási, L. Rosivall, J. Szebeni, L. Dézsi, Paradoxical rise of hemolytic complement in the blood of mice during zymosan- and liposome induced CARPA: a pilot study, Eur. J. Nanomed. 7 (2015) 257–262.

[29] J. Szebeni, P. Bedocs, D. Csukas, L. Rosivall, R. Bunger, R. Urbanics, A porcine model of complement-mediated infusion reactions to drug carrier nanosystems and other medicines, Adv. Drug Deliv. Rev. 64 (2012) 1706–1716.

[30] J. Szebeni, P. Bedocs, R. Urbanics, R. Bunger, L. Rosivall, M. Toth, Y. Barenholz, Prevention of infusion reactions to PEGylated liposomal doxorubicin via tachyphylaxis induction by placebo vesicles: a porcine model, J. Control. Release 160 (2012) 382–387.

[31] R. Urbanics, J. Szebeni, Lessons learned from the porcine CARPA model: constant and variable responses to different nanomedicines and administration protocols, Eur J. Nanomed. 7 (2015) 219–231.

[32] P.P. Wibroe, A.C. Anselmo, P.H. Nilsson, A. Sarode, V. Gupta, R. Urbanics, J. Szebeni, A.C. Hunter, S. Mitragotri, T.E. Mollnes, S.M. Moghimi, Bypassing adverse injection reactions to nanoparticles through shape modification and attachment to erythrocytes, Nat. Nanotechnol. 12 (2017) 589–594.

[33] J. Szebeni, F.M. Muggia, C.R. Alving, Complement activation by Cremophor EL as a possible contributor to hypersensitivity to paclitaxel: an in vitro study, J. Natl. Cancer Inst. 90 (1998) 300–306.

[34] J. Szebeni, L. Baranyi, S. Savay, H.U. Lutz, E. Jelezarova, R. Bunger, C.R. Alving, The role of complement activation in hypersensitivity to pegylated liposomal doxorubicin (Doxil*), J. Liposome Res. 10 (2000) 467–481.

[35] J. Szebeni, C.R. Alving, S. Savay, Y. Barenholz, A. Priev, D. Danino, Y. Talmon, Formation of complement-activating particles in aqueous solutions of Taxol: possible role in hypersensitivity reactions, Intern. Immunopharm. 1 (2001) 721–735.

[36] J. Szebeni, L. Baranyi, S. Savay, J. Milosevits, R. Bunger, P. Laverman, J.M. Metselaar, G. Storm, A. Chanan-Khan, L. Liebes, F.M. Muggia, R. Cohen, Y. Barenholz, C.R. Alving, Role of complement activation in hypersensitivity reactions to doxil and hynic PEG liposomes: experimental and clinical studies, J. Liposome Res. 12 (2002) 165–172.

[37] A. Chanan-Khan, J. Szebeni, S. Savay, L. Liebes, N.M. Rafique, C.R. Alving, F.M. Muggia, Complement activation following first exposure to pegylated liposomal doxorubicin (Doxil): possible role in hypersensitivity reactions, Ann. Oncol. 14 (2003) 1430–1437.

[38] B. Romberg, J.M. Metselaar, L. Baranyi, C.J. Snel, R. Bunger, W.E. Hennink, J. Szebeni, G. Storm, Poly(amino acid)s: promising enzymatically degradable stealth coatings for liposomes, Int. J. Pharm. 331 (2007) 186–189.

[39] J.M. van den Hoven, R. Nemes, J.M. Metselaar, B. Nuijen, J.H. Beijnen, G. Storm, J. Szebeni, Complement activation by PEGylated liposomes containing prednisolone, Eur. J. Pharm. Sci. 49 (2013) 265–271.

[40] G.T. Kozma, T. Mészáros, Z. Weiszhár, T. Schneider, A. Rosta, R.-. Urbanics, L. Rosivall, J.-. Szebeni, Variable association of complement activation by rituximab and paclitaxel in cancer patients in vivo and in their screening serum in vitro with clinical manifestations of hypersensitivity: a pilot study, Eur. J. Nanomed. 7 (2015) 289–301.

[41] L.W. Starmans, D. Burdinski, N.P. Haex, R.P. Moonen, G.J. Strijkers, K. Nicolay, H. Grull, Iron oxide nanoparticle-micelles (ION-micelles) for sensitive (molecular) magnetic particle imaging and magnetic resonance imaging, PLoS One 8 (2013) e57335.

[42] C.W. Jung, P. Jacobs, Physical and chemical properties of superparamagnetic iron oxide MR contrast agents: ferumoxides, ferumoxtran, ferumoxsil, Magn. Reson. Imaging 13 (1995) 661–674.

[43] V. Filipe, A. Hawe, W. Jiskoot, Critical evaluation of nanoparticle tracking analysis (NTA) by NanoSight for the measurement of nanoparticles and protein aggregates, Pharm. Res. 27 (2010) 796–810.

[44] G. Milosevits, Z. Rozsnyay, G.T. Kozma, J. Milosevits, G. Tömöry, H. Robotka, L. Rosivall, J. Szebeni, Flow cytometric analysis of supravesicular structures in doxorubicin-containing pegylated liposomes, Chem. Phys. Lipids 165 (2012) 482–487.

[45] V.P. Ferreira, A.P. Herbert, C. Cortés, K.A. McKee, B.S. Blaum, S.T. Esswein, D. Uhrín, P.N. Barlow, M.K. Pangburn, D. Kavanagh, The binding of Factor H to a complex of physiological polyanions and C3b on cells is impaired in atypical hemolytic uremic syndrome, J. Immunol. 182 (2009) 7009–7018.

[46] T. Shen, R. Weissleder, M. Papisov, A. Bogdanov Jr., T.J. Brady, Monocrystalline iron oxide nanocompounds (MION): physicochemical properties, Magn. Reson. Med. 29 (1993) 599–604.

[47] M.G. Harisinghani, J. Barentsz, P.F. Hahn, W.M. Deserno, S. Tabatabaei, C.H. van de Kaa, J. de la Rosette, R. Weissleder, Noninvasive detection of clinically occult lymph-node metastases in prostate cancer, N. Engl. J. Med. 348 (2003) 2491–2499.

[48] FDA, Postmarketing Safety Review, https://www.fda.gov/ohrms/dockets/ac/05/briefing/2005-4095B1_02_15-FDA-Tab-7-10.pdf, (2005).